Boron−Nitrogen (BN) Substitution Patterns in C/BN Hybrid Fullerenes: $C_{60-2x}(BN)_x$ ($x = 1-7$)

Jayasree Pattanayak, Tapas Kar,* and Steve Scheiner

Department of Chemistry and Biochemistry, Utah State University, Logan, Utah 84322-0300

Received: April 12, 2001

Semiempirical AM1 and MNDO and density functional theory (B3LYP/3-21G and 6-31G*) are used to examine the relative stability of various isomers of successive BN substituted fullerenes $C_{60-2x}(BN)_x$, where x=1−7. It is found that stability is enhanced by keeping BN units and BN filled hexagons adjacent to one another. Successive BN substitution prefers N site attachment to the existing BN chain. The localization of MOs shows that lone-pairs of nitrogen atoms reside "inside" the cage, which may be the reason for outward displacement of N atoms. Geometric parameters and charge distribution of the carbon region of hybrid fullerenes are not much perturbed by BN substitution. Band gap (HOMO−LUMO gap), ionization potential, and electron affinities strongly depend on the number of BN units and filling of the hexagons. Partially BN filled hexagons or unsaturated BN fullerenes have a stronger effect than completely filled hexagons on perturbing these properties.

Introduction

The discovery of fullerenes as stable carbon clusters[1−5] has attracted increasing attention toward similar types of cage-structured compounds with different doping species, containing foreign atoms inside the cage. The other modification of fullerenes involved substitution of carbon atoms by other elements, such as boron and nitrogen. Synthesis and theoretical investigations of the B, N, and BN substituted fullerenes[6−12] have opened a new window into the field of multicomponent fullerenes with more fundamental questions about their stability, morphology, electronic behavior, and basic features of chemical bonding. Several kinds of semiconductors can be expected from BCN materials. One is an intrinsic type of semiconductor which can be converted to a p-type or an n-type extrinsic semiconductor by replacing C by B and N, respectively.

Because of the isoelectronic relationship between boron−nitrogen and carbon−carbon, the BN clusters and BN substituted fullerenes have been the subject of numerous experimental and theoretical studies.[13−24] The structural chemistry of boron nitride closely parallels that of carbon. For example, pure BN is primarily found in hexagonal h-BN (α-BN) form that resembles graphite, sphalerite c-BN (β-BN) is related to cubic diamond, and wurtzite type γ-BN is related to hexagonal diamond.

It was predicted[6] that BN analogues of fullerene would not be stable because N−N and B−B bonds would be required in the molecule, and such bonds are believed to be destabilizing.[6,23] Theoretical investigations[23] using MNDO predict that isomers with small numbers of B−B and N−N bonds are stable by more than 200 kcal/mol compared to those having more such bonds. The same investigation and simple Hückel calculation[13] indicated that $C_{12}B_{24}N_{24}$ (best known as CBN ball) is more stable than C_{60}. However, the opposite result is predicted[25] by nonlocal density functional calculations. The structure of CBN ball, optimized by a non-SCF-MO method using a Harris functional approximation, is distorted by at most 5% from that of C_{60}. Several other theoretical investigations[14,17,26,27] on cagelike structures with general formula $C_{60-(n+m)}B_nN_m$ predict that these species should be stable. The stepwise replacement of CC units of C_{60} with BN can produce $C_{58}BN$, $C_{56}(BN)_2$, etc, and finally, $B_{30}N_{30}$. However, in that case the truncated icosahedral structure is expected to have limited stability because of formation of weak B−B and N−N bonds. It has been shown[14,16,22,28] that to avoid such bonds in BN fullerenes, square rings and hexagons are essential to get a closed structure instead of pentagon−hexagon combination of fullerenes.

The single BN substituted C_{60} molecule $C_{58}BN$ has been examined by several groups[19,23,24,29] using semiempirical approaches. The structure with a BN bond between two hexagons is predicted to be most stable, compared to those having the BN in a fusion position on a hexagon−pentagon border, or structures where B and N atoms are disconnected. The simplest explanation of the preference of B and N atoms to be bonded together is the formation of a dative bond between them. Zhao and co-workers [30,31] extended the study of BN substituted fullerenes by considering $C_{60-2x}(BN)_x$ and $C_{70-2x}(BN)_x$ (x = 1−2), using semiempirical AM1 and MNDO theories to predict their structure, stability, and electronic properties. On the basis of the results of $C_{58}BN$ and $C_{56}(BN)_2$, they proposed the structure of $C_{54}(BN)_3$ where all three BN groups are located in the same six-membered ring. Both AM1 and MNDO predict that substituted fullerenes have considerable stability though less so than their all-carbon analogues. They also found that the most stable structures contain the smallest number of BC and NC bonds.

Although no trend in band gap (HOMO−LUMO gap) was found, substituted fullerenes in general have slightly smaller gaps than pure fullerenes. The band gap of CBN ball (where 24 −CC− units are replaced by −BN− groups) is much larger than that of its parent C_{60}[25], and BN systems are well-known insulators. Such trends in HOMO−LUMO gap are also found in BN substituted small hydrocarbon systems, such as borazine and BN naphthalene.[32] However, partial substitution of C_6H_6 by BN groups lowers the gap compared to the hydrocarbon. In

* Corresponding author: tapaskar@cc.usu.edu, tel 1-435-797-7230.

10.1021/jp011391m CCC: $20.00
Published on Web 08/16/2001

contrast, the band gap increases slowly as more and more CC pairs of naphthalene are replaced by BN. A sharp rise[32] in band gap is noticed beyond third replacement, and it is highest for $B_5N_5H_8$, where BN groups replace all CC units. These results indicate that substitution of pure carbon systems by isoelectronic BN units substantially alter the band gap, and this change strongly depends on the number of BN groups.

Since the previous investigations on BN substituted fullerenes are limited to a small number of BN pairs, no definite conclusion on the general pattern of substitution and properties of such cage systems can be drawn from such studies. It is necessary to extend the number of BN groups in C/BN fullerenes to get a clear picture of substitution effects on pure C_{60}. It will also be interesting to explore whether the substitution patterns observed earlier are true also for the higher ($x > 2$) cases and to identify the additional factors that influence the higher degrees of BN replacement. With these objectives in mind, we extended the study of hybrid C/BN fullerene by considering four to seven BN substituted C_{60} fullerenes, namely, $C_{60-2x}(BN)_x$ where $x = 4-7$. In previous investigations,[31] multiple BN substitutions were restricted only to the six−six ring junctions of fullerenes. However, the most stable structure of $C_{12}B_{24}N_{24}$ consists of BN groups also in six−five ring junctures. To explore such possibilities, $C_{56}(BN)_2$ and $C_{54}(BN)_3$ are also included in the present list of C/BN fullerenes with BN groups in such six−five junctions.

Method of Calculations

Preliminary investigations were carried out using AM1[33] and MNDO [34] methods. Geometries of all systems were fully optimized without any symmetry constraints at these levels. Vibrational analyses at the MNDO level indicate that all isomers of 2−7 BN substituted C_{60} considered in the present investigation have no imaginary frequencies, indicating a true minimum. Energetically favored species thus obtained were subsequently treated at higher levels using density functional theory (DFT). Previous investigations[35−37] on small C/BCN/BN systems indicate the importance of electron correlation for the structure and stability. The density functional theory (DFT)[38−40] method is generally superior to HF, comparable in accuracy to the MP2 method, but less accurate than more extensive correlated methods such as CCSD. However, for systems with large numbers of atoms and moderate basis functions, DFT is more efficient than any other methods that include electron correlation. In the present investigation, DFT calculations were performed using hybrid functionals containing HF exchange and electron correlation terms. Specifically, we used the three-parameter empirical formulation devised by Becke,[41] B3LYP. Although several approximate expressions are available for exchange−correlation functional, B3LYP method is most widely used[42] in the calculation of molecular electronic structure and energetics. For the sake of comparison, additional calculations are performed using the Perdew−Wang functionals for exchange and correlation (pw91pw91).[43] The first three to five most stable isomers obtained at AM1 and MNDO levels were then selected for study by the B3LYP/3-21G method, using MNDO optimized geometries. Finally, the properties of the most stable isomers of each group were calculated using B3LYP/6-31G* method. Such a basis set has been found quite adequate[32,36,37] for present systems. Geometries of 1- and 2-BN fullerenes are also optimized at B3LYP/3-21G and pw91pw91/3-21G levels to verify the reliability of B3LYP/3-21G results using MNDO optimized geometries.

The bonding characteristics of the most stable isomers of C/BN fullerenes were examined using bond-index analysis[44−47] and Boys' localized molecular orbitals (LMOs)[48] at the B3LYP/3-21G method. The positions of the charge centroids in the molecule are used to identify[49,50] the bonds (two and three center) and lone pairs (LPs). Besides bond indices, Mulliken atomic charges[51,52] have also been calculated at both B3LYP/3-21G and B3LYP/6-31G* levels.

Band gaps have been estimated from the energy difference between the highest occupied (HOMO) and the lowest unoccupied (LUMO) molecular orbitals. It is worth mentioning that DFT orbitals are best termed Kohn−Sham (KS) orbitals. Very recently, it has been shown by Stowasser and Hoffmann[53] that the shape and symmetry of the KS orbitals are quite similar to those of the Hartree−Fock (HF) orbitals which chemists are most familiar with. The similarity between KS and HF orbitals has also been reported in several articles.[54−56] These studies indicate that Koopmann's theorem, originally based on Hartree−Fock (HF) orbitals, can be used for KS orbitals to estimate ionization potential (IP) and electron affinity (EA). MNDO and DFT calculations were performed using Gaussian98 program,[57] and MOPAC97 (implemented in CambridgeSoft Chem 3D package) is used for AM1.

Results and Discussion

For the sake of simplicity and to avoid three-dimensional figures, Schlegel's diagram of C_{60} has been used in the present investigation. In this diagram (Figure 1), not only the position of 60 carbon atoms are shown, but also 12 pentagons and 20 hexagons are numbered as Pn ($n = 1-12$) and Hm ($m = 1-20$), respectively. For the description of different isomers, hexagons and pentagons of the Schlegel diagram, where CC units are replaced by BN moieties and their neighboring rings, are shown in Figures 2 to 7. It should be kept in mind that each pentagon is surrounded by five hexagons, and alternate pentagons and hexagons border on each hexagon of fullerenes. Since B−B and N−N bonds are disfavored, such arrangements were avoided while devising different isomers. Moreover, only those isomeric forms where B and N atoms are adjacent were considered because this arrangement is more stable than those where those atoms are disconnected.[23,29] To verify previous MNDO results, we optimized the geometries of the three isomers (**1**−**1** to **1**−**3** of Figure 2) of 1-BN at B3LYP/3-21G and pw91pw91/3-21G methods. In addition to that, B3LYP/3-21G and pw91pw91/3-21G relative energies using MNDO optimized geometries are also provided in parentheses. Although relative energies are sensitive to different methods, their trend is same for all methods. These results (also see 2-BN energies in Figure 2) indicate that MNDO geometries as a prelude to the B3LYP method will provide reliable estimatation of relative energies for BN/C systems.

Relative energies (E_{rel}) of several isomers of three to six BN fullerenes computed at AM1, MNDO, and B3LYP/3-21G//MNDO levels are summarized in Figures 3−6 along with their structural arrangements. Two integers have been used to identify those isomers. The first integer indicates the number of CC units replaced, and the second corresponds to a number assigned to each isomer. In all cases, the relative energy of the most stable isomer of each group is defined as zero, and less stable isomers are arranged in increasing order of E_{rel}.

It can be seen from Figures 3−6 that E_{rel} values are sensitive to the level of calculations. However, the trends are in general similar in all three methods. It is stressed that we are not focused so much on the accuracy of the energy values or other properties but rather on trends. We will mainly focus on DFT/6-31G* results wherever calculated, otherwise MNDO.

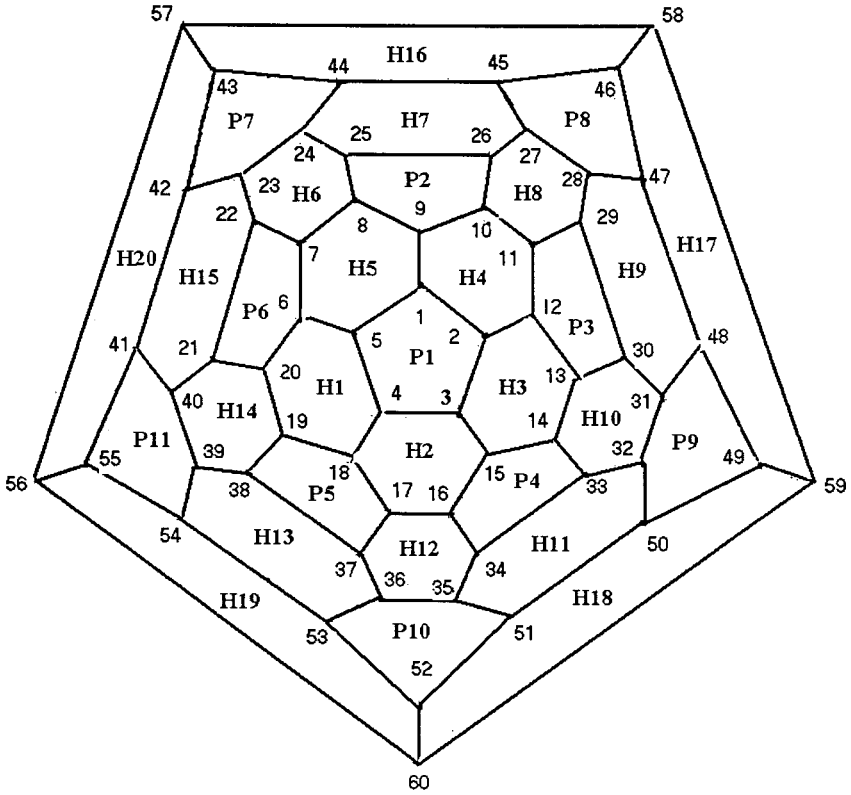

Figure 1. Schlegel diagram of C_{60}. **H** and **P** represent hexagons and pentagons, respectively.

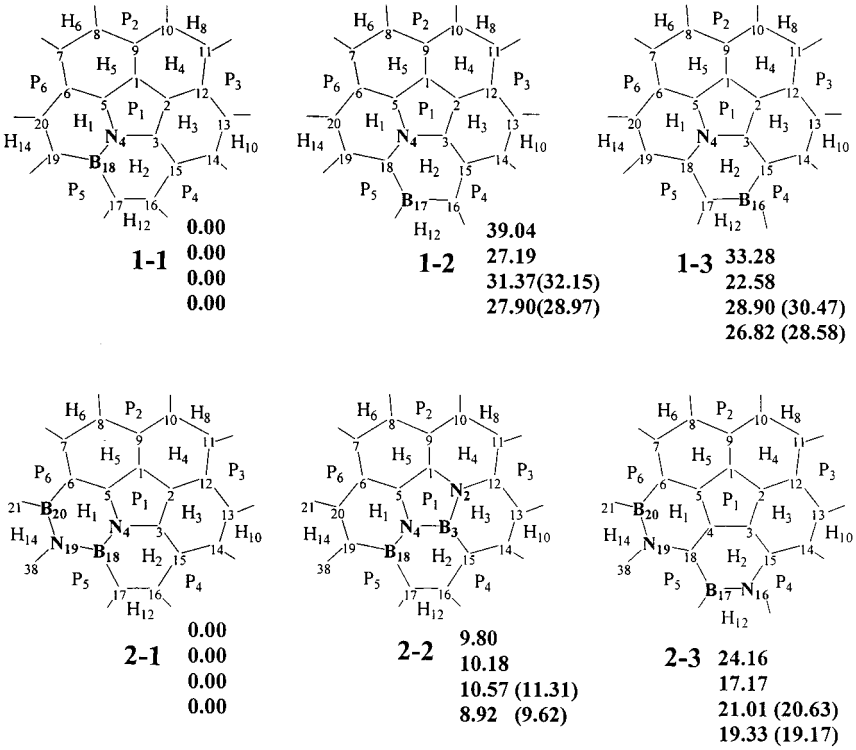

Figure 2. Isomers of 1-BN and 2-BN fullerenes with relative energies (E_{rel} in kcal/mol). E_{rel} values are listed in the order of AM1, MNDO, B3LYP/3-21G, and pw91pw91/3-21G. Geometries are optimized at the same level of theory. Values in parentheses correspond to DFT energies using MNDO optimized geometries. Only the relevant sections of the entire fullerenes are shown. B and N atoms are drawn in bold. Same numbering scheme of the atoms and rings are maintained in this and figures 3−7.

A. Energetics. In the case of single BN substitution, the preferred site[31] for BN is 6−6 (i.e., junction of six−six rings) position as illustrated by **1**−**1** in Figure 2. Since replacement of second carbon pairs in all possible six−six ring joints have already been reported,[31] we only consider some hexagon−pentagon joints (6−5 positions) by keeping the first BN unit in its preferred 6−6 site (**1**−**1** in Figure 2). All of such arrangements are unstable compared to the global minimum **2**−**1** in Figure 2 (only three isomers are shown here) where BN groups are adjacent, head-to-tail. Note that the BN bonds in **2**−**1** represent H−H, H−P, and H−H junctions. Other isomers where the second BN group is attached to the first one and located in

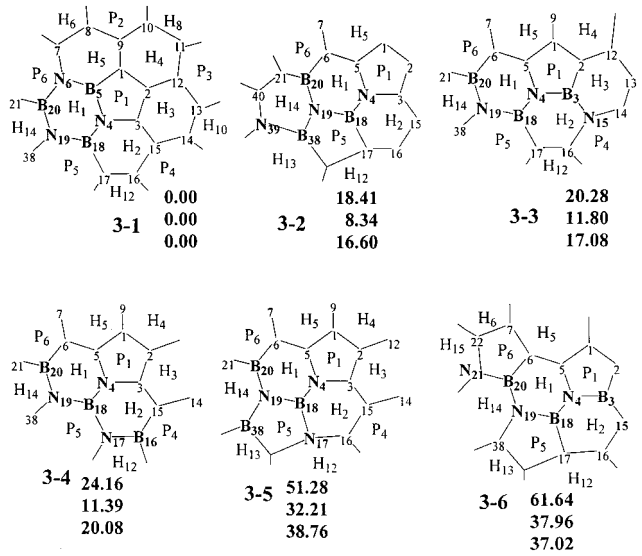

Figure 3. Isomers of 3-BN fullerenes with relative energies (E_{rel} in kcal/mol). E_{rel} values are listed in the order of AM1, MNDO, and B3LYP/3-21G//MNDO.

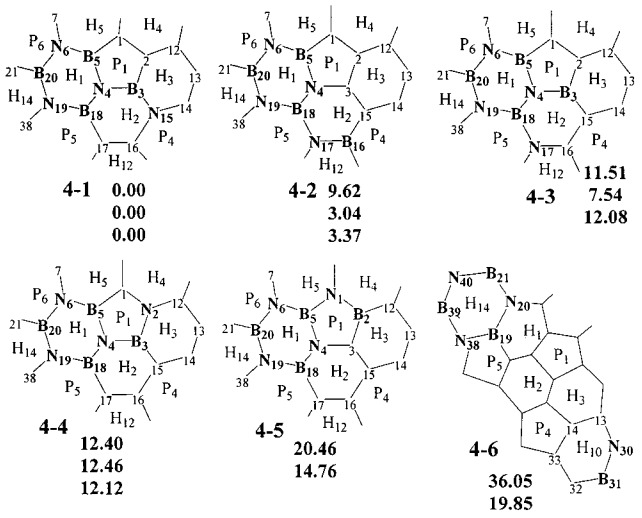

Figure 4. Isomers of 4-BN fullerenes with relative energies (E_{rel} in kcal/mol). E_{rel} values are listed in the order of AM1, MNDO, and B3LYP/3-21G//MNDO.

any of the pentagon−hexagon (5−6) junctions are less stable by more than 9 kcal/mol. Even higher in energy by more than 10 kcal/mol are isomers where BN units are separated by one (**2**−**3**) or more C atoms. These results indicate that 6−5 positions are not favorable as long as 6−6 counterparts are available for replacement. The other crucial factor for the stability of BN/C systems is the consecutiveness of BN units, which results in additional BN bonds connecting them. (It may be noted that those bonds are in general located at pentagon−hexagon junctions because of geometric arrangements of fullerenes). Formation of extra BN bonds enhances the stability of the system because such bonds are most stable of all bond types involved in B/C/N molecules. For example, the experimental cohesive energy of a B−N bond is highest (4.00 eV) when compared to C−C (3.71), B−C (2.59), N−C (2.83), B−B (2.32), and N−N (2.11).[58]

Six possible isomers of 3-BN fullerene obtained by replacing a third CC pair, starting from **2**−**1,** are summarized in Figure 3. In general, isomers where the third BN unit is not connected to the first two pairs or spread over pentagon−hexagon junctions are quite unstable and hence omitted from the figure. As predicted by Chen et al.,[31] the most stable isomer (**3**−**1)** places all six heteroatoms in the same ring. In this isomer, the number of BN bonds is maximum (six), compared to only five in the others. The remaining 3-BN isomers shown in Figure 3, with the same number (five) of BN bonds, show a wide difference in relative energies. They can be categorized into groups depending on the BN positions, and the stability of each group member is within a close range. For example, isomers **3**−**2** to **3**−**4** are within 5 kcal/mol of one another, and all contain BN in three H−H junctions and two H−P junctions. All three methods predict lowest energy of **3**−**2** where N_{19} is surrounded by three B atoms. Thus, it seems the N-site substitution is more favorable compared to B-site as in **3**−**4**. In the next few sections, it will be shown that this feature is retained for higher substituted BN fullerenes. This important substitution pattern has not been reported previously.

In both **3**−**2** and **3**−**3,** the third BN is attached to the N-site, but in the former it forms a branch chain of BN, while a continuous −BNBNBN− chain is formed in the latter structure. These two isomers are almost isoenergetic (see DFT/3-21G values). However, if 5−6 positions are involved in the continuous (as in **3**−**6**) or branch (**3**−**5)** −BN− chains, energy is further raised by 20 kcal/mol. **3**−**5** and **3**−**6** both contain 2 H−H and 3 H−P junctions yielding higher energies. We have also noticed that much higher E_{rel} values (not shown in Figure 3) is associated with increasing number of the intervening −CC− bonds or rings between BN pairs even though they are in preferred 6−6 joints.

Upon determining the most stable structure of 3-BN fullerenes, we proceed to the next higher BN fullerenes by maintaining those simple rules of substitution found in smaller BN fullerenes. The most preferred structure **4**−**1** (see Figure 4) of 4-BN fullerene is obtained as a derivative of **3**−**1** by adding a BN pair to an N atom of the H_1 ring. As observed previously, adding a BN to a B atom of the ring (**4**−**2**) is less stable by some 3 kcal/mol than addition to the N-site. A similar energy difference (∼ 2 kcal/mol) is found between **4**−**4** and **4**−**5**. The latter two structures differ from **4**−**1** and **4**−**2** in that both of the extra-ring BN bonds occur on P−H junctions. These two isomers are comparable in energy to **4**−**3** where the added B and N atoms are separated. Even less stable is the isomer **4**−**6** when the last BN unit removed from the full BN ring, placed in a different hexagon faced toward the first ring in three dimension.

Figures 5 and 6 summarize the structures and energy results of 5- and 6-BN fullerenes, respectively. In the former case, the most stable structure consists of two completely filled hexagons H1 and H2. The next BN pair goes preferentially to substitution of an N atom to form **6**−**1**. Any other isomers in 5-BN fullerene are much higher in energy because they differ from the filled ring motif. **6**−**2** is not much higher in energy than **6**−**1** as both contain two filled rings. It is interesting to note that when two hexagons are completely occupied as in **6**−**4** and **6**−**5**, the ensuing structure is higher by more than 25 kcal/mol because of the separation of these two hexagons. The findings of 2- to 6-BN fullerenes clearly predict that the next substitution will continue to fill a third hexagon to form 7-BN fullerene as shown in **7**−**1** in Figure 7. From figures 3 to 6, it can be seen that the energy difference between the global minimum and the next stable isomer is substantially higher in fully occupied 3- and 5-BN fullerenes than in their partially filled 4 and 6 counterparts. The extra stability of the former arrangements may be due in part to minimal distortion of the carbon networks by BN replacement.

B. Structure and Nature of Bonding. Several theoretical and experimental structures of C_{60} have been reported,[3] and the

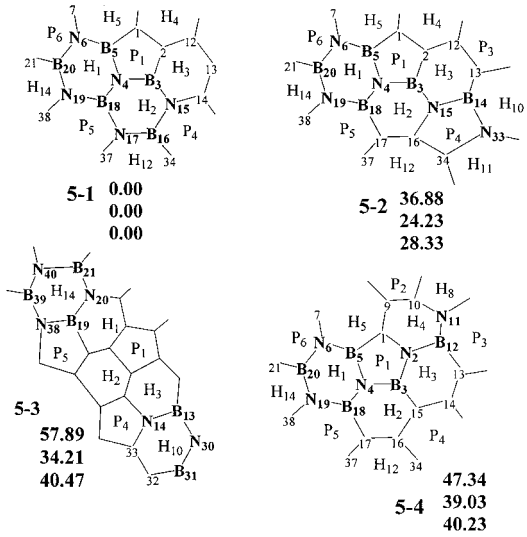

Figure 5. Isomers of 5-BN fullerenes with relative energies (E_{rel} in kcal/mol). E_{rel} values are listed in the order of AM1, MNDO, and B3LYP/3-21G//MNDO.

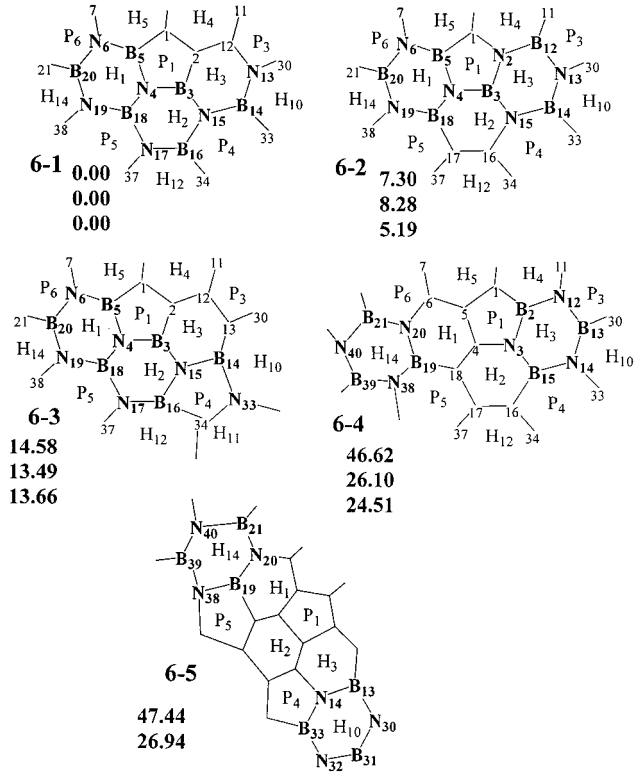

Figure 6. Isomers of 6-BN fullerenes with relative energies (E_{rel} in kcal/mol). E_{rel} values are listed in the order of AM1, MNDO, and B3LYP/3-21G//MNDO.

MNDO geometries are in good agreement with more accurate theoretical methods and experimental values. The CC bond lengths in 6−6 and 6−5 linkages of C_{60} are 1.400 and 1.474 Å, respectively. BN substitution distorted the geometric parameters of C_{60} only in their immediate vicinity leaving the rest of the fullerene's geometry almost unchanged. Similar to CC distances, different BN lengths at 6−6 and 6−5 positions are predicted by MNDO theory. BN bonds in the former positions (1.450 ± 0.004 Å) are shorter than those located in 6−5 positions (1.485 ± 0.006 Å). The BN bond lengths are less sensitive to position than are CC bonds in C_{60}. The BC and NC bond lengths lie between 1.46 to 1.55 Å and 1.44 to 1.45 Å, respectively. A wavelike or rippled surface of BN nanotubes,

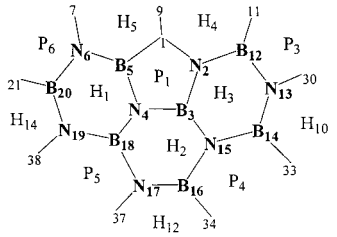

Figure 7. Structure of the 7-BN fullerene.

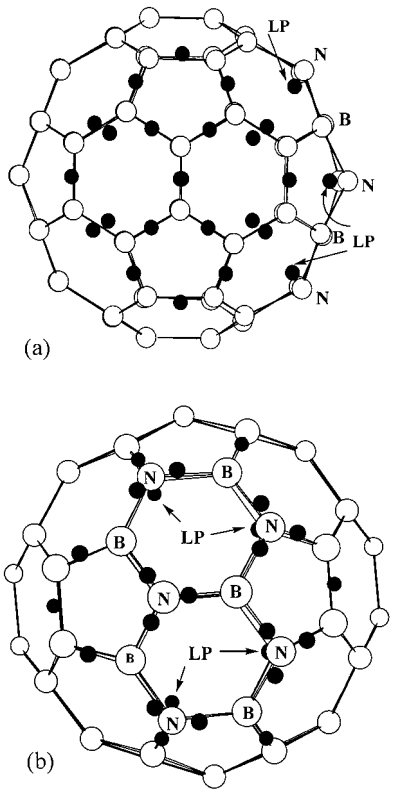

Figure 8. Localized Molecular orbitals (LMOs) of 5-BN fullerene. Black dots indicate the positions of the charge centroids. Each LMO charge centroid represents a pair of electrons. LMOs of 5-BN fullerene at different angles are shown in (a) and (b) from different perspectives.

with B atoms displaced inward and N atoms moved outward, has been noted by Menon and Srivastava.[28] We also found such geometric distortion in the partially substituted BN fullerenes (for example, see Figure 8a where three N atoms of 5-BN fullerene bulge slightly outward). The BNB and NBN bond angles also deviate by 2−4° from the ideal 120° of θ(CCC) in C_{60}. Sharper BNB and wider NBN bond angles are also associated with small BC_2N molecules.[36,37]

Because of electronegativity differences between boron, nitrogen, and carbon atoms, atomic charges are nonzero in the BN fullerenes. Atomic charges calculated by density functional theory using 3-21G and 6-31G* basis set are reported in Table 1. (Carbon atoms with atomic charge less than ±0.02 are not tabulated.) DFT/3-21G charges are in general larger in magnitude than 6-31G*. It can be seen that only those carbons attached to the heteroatoms possess appreciable charge, that is, C atoms are positively or negatively charged depending on their attachments with N or B atoms, respectively. These C charges, especially when negative, are significantly smaller than those of the B and N atoms to which they are attached. The charge distributions of BN fullerenes are almost independent of the number of BN groups. For example, the 6-31G* charge of N_4

TABLE 1: Total Atomic Charges[a] (B3LYP/3-21G (A) and B3LYP/6-31G* (B)) of the Most Stable Isomers of 1BN−7BN

atom's positi on[b]		atoms	1BN		2BN		3BN		4BN		5BN		6BN		7BN	
			A	B	A	B	A	B	A	B	A	B	A	B	A	B
1	P1	C					−0.33	−0.07	−0.32	−0.07	−0.32	−0.07	−0.32	−0.07	−0.10	0.10
2		C/N							−0.32	−0.07	−0.32	−0.07	−0.32	−0.07	**−0.75**	**−0.48**
3		C/B	0.25	0.20	0.20	0.17	0.20	0.17	**0.93**	**0.42**	**0.91**	**0.39**	**0.88**	**0.37**	**0.88**	**0.53**
6		C/N			−0.31	−0.06	**−0.76**	**−0.48**	**−0.82**	**−0.46**	**−0.83**	**−0.48**	**−0.83**	**−0.48**	**−0.83**	**−0.48**
18		B	**1.02**	**0.29**	**0.99**	**0.28**	**0.97**	**0.41**	**0.91**	**0.39**	**0.91**	**0.39**	**0.91**	**0.39**	**0.88**	**0.37**
4	H1	N	**−0.72**	**−0.50**	**−0.75**	**−0.46**	**−0.76**	**−0.48**	**−0.76**	**−0.48**	**−0.76**	**−0.48**	**−0.77**	**−0.48**	**−0.76**	**−0.48**
20		C/B			**0.99**	**0.44**	**0.97**	**0.41**	**0.97**	**0.41**	**0.96**	**0.41**	**0.96**	**0.41**	**0.96**	**0.41**
19		C/N	−0.31	−0.06	**−0.72**	**−0.52**	**−0.76**	**−0.48**	**−0.76**	**−0.48**	**−0.77**	**−0.49**	**−0.77**	**−0.49**	**−0.77**	**−0.49**
5		C/B	0.25	0.20	0.21	0.17	**0.97**	**0.41**	**0.93**	**0.40**	**0.91**	**0.54**	**0.91**	**0.54**	**0.91**	**0.54**
17	H2	C/N	−0.31	−0.06	−0.32	−0.06	−0.33	−0.07	−0.33	−0.07	**−0.77**	**−0.49**	**−0.77**	**−0.49**	**−0.77**	**−0.49**
16		C/B							0.21	0.17	**0.96**	**0.41**	**0.91**	**0.38**	**0.90**	**0.38**
15		N							**−0.72**	**−0.52**	**−0.76**	**−0.78**	**−0.82**	**−0.46**	**−0.84**	**−0.48**
14	H3	C/B							0.24	0.20	0.19	0.17	**0.93**	**0.41**	**0.91**	**0.39**
13		N											**−0.72**	**−0.52**	**−0.76**	**−0.48**
12		C/B											0.21	0.17	**0.95**	**0.40**
11	H4	C													−0.32	−0.07
9		C													−0.05	−0.02
7	H5	C					0.20	0.17	0.20	0.17	0.19	0.17	0.19	0.17	0.19	0.16
21	P6	C			−0.32	−0.07	−0.33	−0.07	−0.33	−0.07	−0.33	−0.07	0.33	−0.07	−0.33	−0.07
38	P5	C			0.24	0.20	0.20	0.17	0.20	0.17	0.20	0.17	0.20	0.17	0.20	0.17
37		C									0.20	0.17	0.20	0.17	0.20	0.17
34	H12	C									−0.33	−0.07	−0.32	−0.07	−0.32	−0.07
30	H10	C											0.24	0.20	0.19	0.17
33	P4	C											−0.32	−0.07	−0.32	−0.07

[a] Charges in bold are for B and N atoms, otherwise for C atoms. [b] Position of C, B, and N atoms as described in Figure 1.

is very close to −0.48 for $x = 1-7$. These results indicate that the part of the BN fullerene surface near the heteroatoms contains more highly charged atoms than the rest of the system.

Because of its electron deficient nature, boron is typically involved in three-center bonds. BNB, BCC, and CCC three-center two-electron bonds and NBN, NCC, and CCC three-center four-electron bonds have been identified [36,37] in small BC_2N systems. No such three-center bonds have been found in the present fullerene molecules. The localized molecular orbital (LMO) studies show that electron pairs are perfectly localized on bonds and lone pairs (LPs). LMOs of 5-BN fullerene, as a representative case, are illustrated in Figure 8. For the sake of clarity, lone pairs of nitrogen atoms and bond pairs located in a few 6−6 and 6−5 junctions are illustrated in those figures by filled black circles. As expected, each pentagon−hexagon connecting bond contains one electron pair, while two electron pairs are located between hexagon−hexagon joints causing different CC and BN bond lengths in C_{60} and BN fullerenes, respectively.

The most striking outcome of the present LMO studies is the position of nitrogen lone pairs. It can be seen from Figures 8a and 8b that nitrogen LPs are located "inside" the cage structure, which may be responsible for the outward motion of N atoms in BN fullerenes. Thus, BN fullerenes contain more electron density inside the cage than all carbon counterparts, and this feature is enhanced as more BN units are added to fullerenes. Because of the greater electronegativity of N, the center of charge in BN and CN bond pairs is closer to N atom. Similarly, electron pairs are closer to carbon atoms in BC bonds. Thus, the ionic character of different kinds of bonds involved in BN fullerenes is consistent with the positions of the LMOs.

C. HOMO−LUMO Gap, Ionization Potentials, and Electron Affinities. HOMO−LUMO gaps of 1- to 7-BN fullerenes obtained from both semiempirical and density functional theories are plotted against the number of BN units in Figure 9. For the sake of comparison, the HOMO−LUMO gap of C_{60} has also been included on the far left in this figure. Although HOMO−LUMO gaps strongly depend on various methods, their trends

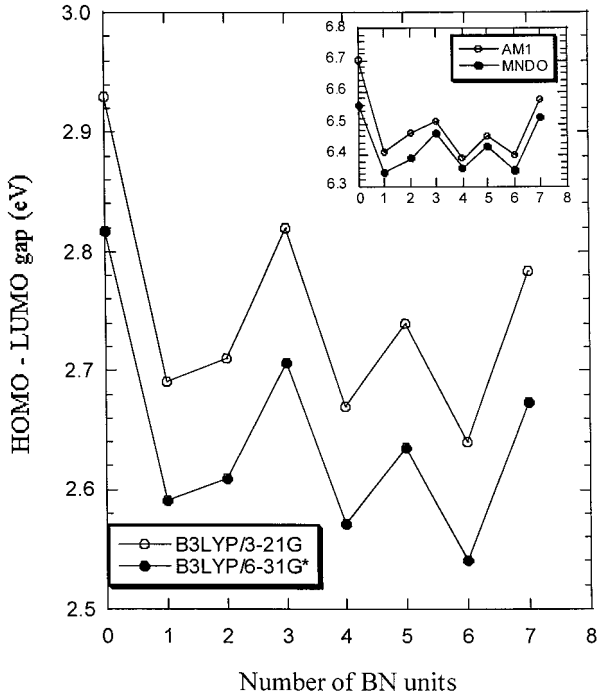

Figure 9. Variation of HOMO−LUMO gaps with the number of BN groups.

are the same. In general, semiempirical gaps in the figure inset are about 2.5 times larger than those of B3LYP/6-31G* values, and this ratio is almost independent of the number of BN units. It can be seen from Figure 9 that all BN fullerenes have a smaller HOMO−LUMO gap than does semiconducting C_{60}. However, the HOMO−LUMO energy difference of heterofullerenes strongly depends on the number of BN pairs. Single BN substitution lowers the band gap of C_{60} by 0.23 eV at DFT/6-31G* level, and a slight increase (0.02 eV) is noticed upon adding a second BN pair. In both cases, hexagons are partially filled by BN units. A sharp rise of 0.10 eV occurs when all three CC pairs of a hexagon are replaced by heteroatom pairs.

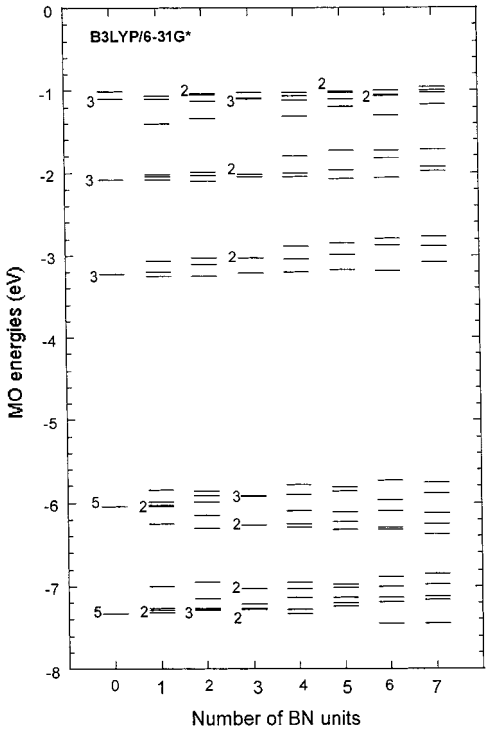

Figure 10. B3LYP/6-31G* MO energies of C_{60} and 1- to 7-BN fullerenes. The numbers beside the MOs represent orbital degeneracy.

This trend in HOMO−LUMO gap also continues to higher BN fullerenes, reaching peaks for 5 and 7 BN pairs. As a general trend, the gap decreases in each series of filled and partially filled BN fullerenes, and the smallest value (2.54 eV) is found in **6**−**1**. On the other hand, 7-BN fullerene has a larger band gap than previous filled **5**−**1,** a turning point observed in this pattern. This reversal is not unexpected since $C_{12}B_{24}N_{24}$ (24-BN fullerene) has a much larger gap than does fullerene.[19]

To analyze the changes in HOMO−LUMO gap and the effect of BN substitution on the orbital energies near the Fermi level, 10 occupied and 10 unoccupied orbital energies obtained from B3LYP/6-31G* calculations are presented in Figure 10. The number beside each MO represents the orbital degeneracy. The 5-fold degeneracy of the HOMO and SHOMO and the 3-fold degeneracy of LUMO, LUMO+1, and LUMO+2 of C_{60} are lifted as BN pairs are added because of the lower symmetry of BN fullerenes. This splitting continues as more BN units are added. In general, both increase and decrease of bonding character is found for occupied MOs, which are both above and below their unsubstituted fullerene counterparts. However, the unoccupied MOs of BN fullerenes exhibit more antibonding nature than in C_{60}.

A closer look at MOs reveals that LUMO remains almost constant over the range (except **7**−**1**), whereas the HOMO becomes slightly more antibonding as the number of BN groups increases. Hence, the fluctuations in HOMO energies are mainly responsible for fluctuations in the HOMO−LUMO gaps of 1- to 6-BN fullerenes. It can be seen that HOMOs of completely filled BN hexagons (**3**−**1**, **5**−**1** and **7**−**1**) are lower in energy than those of partially filled hexagons. Traditionally, the HOMO−LUMO gaps are associated with chemical stability against electronic excitations. Larger gaps correspond to greater stability, so one might expect the "filled" hexagons to be most resistant to oxidation. The first singlet vertical excitation energies (C_{60}: 3.34, **1**−**1**: 3.22, **2**−**1**: 3.26, **3**−**1**: 3.36; **4**−**1**; 3.22, **5**−**1**: 3.31; **6**−**1**: 3.15 and **7**−**1**: 3.29 eV) calculated at CIS/3-21G//MNDO level are in accordance with the trends observed in HOMO−LUMO gaps.

DFT/6-31G*//MNDO ionization potentials (IP) and electron affinities (EA) of the most stable isomers of BN fullerenes are shown in Figure 11. The IP curve indicates that substituted fullerenes have somewhat smaller ionization potentials relative to C_{60}, and the trend in IP values is similar to band gap discussed earlier. The continuous decay of ionization potentials confirms the tendency of heterofullerenes to more easily lose an electron (oxidation) with higher substitution. The electron affinity potential also shows stepwise decay (except 1- and 2-BN fullerenes). However, this change in EA is not as pronounced as it is in IP, except for the **7**−**1** structure where three hexagons are completely filled by heteroatoms. In short, the behavior of IP and EA suggests that redox characteristics of fullerenes, $C_{60-2x}(BN)_x$, are enhanced by doping BN groups only up to $x = 2$. Higher BN fullerenes are easier to oxidize but harder to reduce relative to C_{60}.

Conclusion

The pattern of successive substitution of carbon pairs of C_{60} fullerene by isoelectronic BN moieties has been evaluated using density functional and semiempirical theories. Although numerical values differ, trends in structure, stability, and electronic properties obtained from AM1 and MNDO are in good agreement with more accurate DFT (B3LYP/3-21G and B3LYP/6-31G*) methods.

The first carbon pair substitution takes place in a hexagon−hexagon junction (H1−H2 in Figure 1) of C_{60} to form $C_{58}BN$

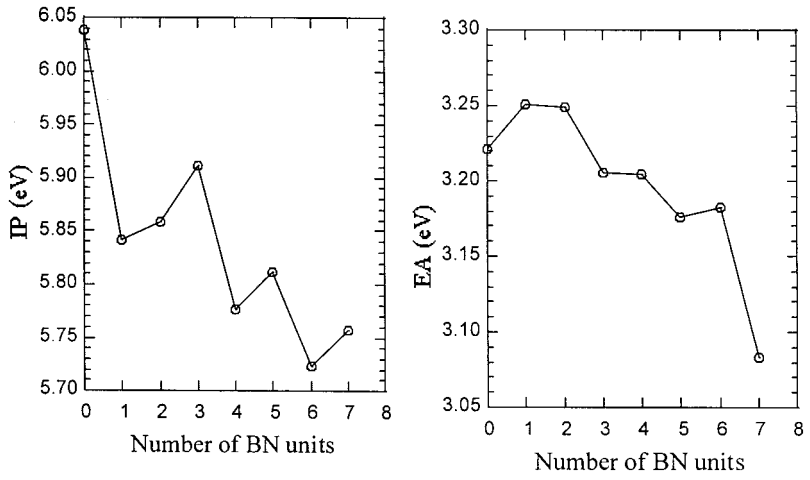

Figure 11. Variation of ionization potential (IP in eV) and electron affinity (EA in eV) with the number of BN units.

or 1-BN fullerene. It may be noted that CC bonds in hexagon−hexagon junctions are shorter (double-bond type) than the corresponding CC bonds (single-bond type) in hexagon−pentagon junctions. Thus, BN substitution prefers a double-bond site rather than single-bonded carbon pairs. This may be due to the easy formation of N → B dative bond.

The next two BN units replace carbons of the same hexagon (H1). In the first two cases, one of the hexagons of C_{60} can be considered as partially BN filled or unsaturated BN fullerenes, while the third one can be termed saturated or fully BN filled fullerene. As we continue replacing CC pairs up to seven pairs, BN units spread to the adjacent hexagons covering one by one from H1 to H2 and finally to H3, with these hexagons surrounding pentagon P1. The most stable isomers of 1- to 7-BN fullerenes contain the maximum number of BN bonds. Another ruling factor of successive BN substitution is that the N-site attachment of the next BN unit to the existing group is more favorable than the B-site. Any other structural arrangement, where BN units are not consecutive or some of the heteroatom pairs are placed in hexagon−pentagon joints or the filling of a pentagon, causes instability. The same is true with the increase in the number of intervening rings between fully BN substituted hexagons.

The present investigation and previous studies on small BCN hybrid systems clearly indicate that stability is enhanced substantially by not only keeping BN units together, but also by a continuity of fully BN filled or saturated hexagons. These results certainly call into question the **Model II** structural

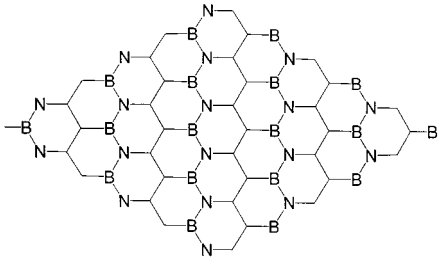

Model II

arrangement with alternate −C−C− and −B−N− chains, which is so far considered[59−62] as the most stable BC_2N structure. In the absence of unambiguous prediction or experimental determination for the atomic arrangements of BC_2N, **Model II** has been used by almost all theoretical works.[63,64]

BN fullerenes exhibit certain characteristics which may be important in the nanotechnology field. The geometric parameters of C_{60} are not much perturbed by BN substitutions, except around the −BNBN− area. Nitrogen atoms are bent outward because of the presence of their lone pairs "inside" the cage structure. Because of the electronegativity differences, part of the BN fullerenes acquire some alternating charges in the heteroatom regions, keeping the rest of the system electrically neutral. The HOMO−LUMO gap of semiconducting C_{60} lowers by substitution, and the effect is more pronounced in unsaturated BN fullerenes. Redox characteristics of C_{60} also strongly depend on the number of BN units in $C_{60-2x}(BN)_x$. It seems BN fullerenes contain dual characteristics: the all-C region and the BN area appear to be different from one another.

References and Notes

(1) Dresselhaus, M. S.; Dresselhaus, G.; Eklunf, P. C. *Science of Fullerenes and Carbon Nanotubes*; Academic Press: New York, 1996.

(2) *Fullerenes and fullerene nanostructures*; Kuzmany, H., Fink, J., Mehring, M., Roth, S., Eds.; World Scientific: Singapore, 1996.

(3) Cioslowski, J. *Electronic Structure Calculations on Fullerenes and their Derivatives*; Oxford University Press: New York, 1995.

(4) *Fullerenes and related structures*; Hirsch, A., Ed.; Springer: Berlin, 1999; Vol. 199.

(5) *Fullerenes and Related Structures*; Hirsch, A., Ed.; Springer: Berlin, 1999; Vol. 199.

(6) Guo, T.; Jin, C.; Smalley, R. E. *J. Phys. Chem.* **1991**, *95*, 4948−4950.

(7) Miyamoto, Y.; Hamada, N.; Oshiyama, A.; Saito, S. *Phys. Rev. B* **1992**, *46*, 1749.

(8) Pradeep, T.; Vijayakrishna, V.; Santra, A. K.; Rao, C. N. R. *J. Phys. Chem.* **1991**, *95*, 1991.

(9) Piechota, J.; Byszewski, P.; Jablonski, R.; Antonova, K. *Fullerene Sci. Technol.* **1996**, *4*, 491−507.

(10) Chen, Z.; Zhao, X.; Tang, A. *J. Phys. Chem. A* **1999**, *103*, 10961−10968.

(11) Kurita, N.; Koboyyashi, N.; Kumabora, H.; Tago, K.; Ozawa, K. *Chem. Phys. Lett.* **1992**, *198*, 95. (a) Kurita, N.; Koboyyashi, N.; Kumabora, H.; Tago, K. *Phys. Rev. B* **1993**, *48*, 4850.

(12) Wang, S. H.; Chen, F.; Fann, Y. C.; Kashani, M.; Malaty, M.; Jansen, S. A. *J. Phys. Chem.* **1995**, *99*, 6801.

(13) Bowser, J. R.; Jelski, D. A.; George, T. F. *Inorg. Chem.* **1992**, *31*, 154−156.

(14) Jensen, F.; Toftlund, H. *Chem. Phys. Lett.* **1993**, *201*, 89−96.

(15) Jensen, H.; Sorensen, G. *Surf. Coat. Technol.* **1996**, *84*, 524−527.

(16) Silaghi-Dumitrescu, I.; Haiduc, I.; Sowerby, D. B. *Inorg. Chem.* **1993**, *32*, 3755−3758.

(17) Silaghi-Dumitrescu, I.; Lara-Ochoa, F.; Bishof, P.; Haiduc, I. *J. Mol. Struct. (THEOCHEM)* **1996**, *367*, 47−54.

(18) Brado, R. D.; T., S. C.; Jones, W. H. *Inorg. Chem.* **1994**, *31*, 154.

(19) Kurita, N.; Kobayashi, K.; Kumahora, H.; Tago, K. *Fullerene Sci. Technol*. **1993**, *1*, 319.

(20) Gao, Y. D.; Herndon, W. C. *J. Am. Chem. Soc.* **1993**, *115*, 8459.

(21) Placa, S. J. L.; Roland, P. A.; Wynne, J. J. *Chem. Phys. Lett.* **1992**, *190*, 163.

(22) Zhu, H.-Y.; Klein, D. J.; Seitz, W. A.; March, N. H. *Inorg. Chem.* **1995**, *34*, 1377−1383.

(23) Xia, X.; Jelski, D. A.; Bowser, J. R.; George, T. F. *J. Am. Chem. Soc* **1992**, *114*, 6493−6496.

(24) Esfarjani, K.; Ohno, K.; Kawazoe, Y. *Phys. Rev. B* **1994**, *50*, 17830−17836.

(25) Kobayashi, K.; Kurita, N. *Phys. Rev. Lett.* **1993**, *70*, 3542.

(26) Alexandre, S. S.; Mazzoni, M. S. C.; Chacham, H. *Appl. Phys. Lett.* **1999**, *75*, 61−63.

(27) Zhu, H.-Y.; Schmalz, T. G.; Klein, D. J. *Int. J. Quantum Chem.* **1997**, *63*, 393−401.

(28) Menon, M.; Srivastava, D. *Chem. Phys. Lett.* **1999**, *307*, 407−412.

(29) Chen, Z.; Ma, K.; Chen, L.; Zhao, H.; Pan, Y.; X., Z.; Tang, A.; Feng, J. *J. Mol. Struct. (THEOCHEM)* **1998**, *452*, 219−225.

(30) Chen, Z.; Ma, K.; Pan, Y.; Zhao, X.; Tang, A. *J. Mol. Struct. (THEOCHEM)* **1999**, *490*, 61−68.

(31) Chen., Z.; Ma, K.; Zhao, H.; Pan, Y.; Zhao, X.; Tang, A.; Feng, J. *J. Mol. Struct. (THEOCHEM)* **1999**, *466*, 127−135.

(32) Kar, T.; Dalmore, D. E.; Scheiner, S. *J. Mol. Struct. (THEOCHEM)* **1997**, *392*, 65−74.

(33) Dewar, M. J. S.; Zoebisch, E. G.; Healy, E. F.; Stewart, J. J. P. *J. Am. Chem. Soc.* **1985**, *107*, 3902−3909.

(34) Dewar, M. J. S.; Thiel, W. *J. Am. Chem. Soc.* **1977**, *99*, 4899−4907.

(35) Martin, J. M. L.; Taylor, P. R. *J. Phys. Chem.* **1994**, *98*, 6105−6109.

(36) Kar, T.; Cuma, M.; Scheiner, S. *J. Phys. Chem. A* **1998**, *102*, 10134−10141.

(37) Kar, T.; Cuma, M.; Scheiner, S. *J. Mol. Struct. (THEOCHEM)* **2000**, *556*, 275−281.

(38) Parr, R. J.; Yang, W. *Density-Functional Theory of Atoms and Molecules*; Oxford University Press: Oxford, 1989.

(39) Dreizler, R. M.; Gross, E. K. U. *Density Functional Theory, An Approach to the Quantum Many Body Problem*; Springer-Verlag: New York, 1990.

(40) *Density Functional Methods in Chemistry*; Labanowski, J. K., Andzelm, J. W., Eds.; Springer-Verlag: New York, 1991.

(41) Becke, A. D. *J. Chem. Phys.* **1992**, *96*, 2155−2160; **1993**, *98*, 5648−5652.

(42) Cohen, A.; Handy, N. C. *Chem. Phys. Lett.* **2000**, *316*, 160.

(43) Burke, K.; Perdew, J. P.; Wang, Y. In *Electronic Density Functional Theory: Recent Progress and New Directions*; Dobson, J. F., Vignale, G., Das, M. P., Eds.; Plenum: 1998. (b) Perdew, J. P. In *Electronic Structure of Solids '91*; Ziesche, P., Eschrig, H., Eds.; Akademie Verlag: Berlin, 1991; p 11. (c) Perdew, J. P.; Chevary, J. A.; Vosko, S. H.; Jackson, K. A.;

Pederson, M. R.; Singh, D. J.; Fiolhais, C. *Phys. Rev.* **1992**, *B46*, 6671. (d) Perdew, J. P.; Chevary, J. A.; Vosko, S. H.; Jackson, K. A.; Pederson, M. R.; Singh, D. J.; Fiolhais, C. *Phys. Rev.* **1993**, *B48*, 4978. (e) Perdew, J. P.; Burke, K.; Wang, Y. *Phys. Rev.* **1996**, *B54*, 16533.

(44) Sannigrahi, A. B. *Adv. Quantum Chem.* **1991**, *23*, 301−351.

(45) Sannigrahi, A. B.; Kar, T. *Chem. Phys. Lett.* **1990**, *173*, 569−572.

(46) Kar, T.; Marcos, E. S. *Chem. Phys. Lett.* **1992**, *192*, 14−20.

(47) Kar, T. *J. Mol. Struct (THEOCHEM)* **1993**, *283*, 313−315.

(48) Boys, S. F. *Quantum Theory of Atoms, Molecules and the Solid State*; Academic Press: 1966.

(49) Kar, T.; Jug, K. *Chem. Phys. Lett.* **1996**, *256*, 201−206.

(50) Kar, T.; Jug, K. *Int. J. Quantum Chem.* **1995**, *53*, 407.

(51) Mulliken, R. S. *J. Chem. Phys.* **1955**, *23*, 1833−1840.

(52) Mulliken, R. S. *J. Chem. Phys.* **1955**, *23*, 1841−1846.

(53) Stowasser, R.; Hoffmann, R. *J. Am. Chem. Soc.* **1999**, *121*, 3414.

(54) Yang, W.; Mortier, W. J. *J. Am. Chem. Soc.* **1986**, *108*, 5708.

(55) Hoffmann, R. *J. Mol. Struct. (THEOCHEM)* **1998**, *424*, 1.

(56) Kar, T.; Angyan, J. G.; Sannigrahi, A. B. *J. Phys. Chem.* **2000**, *104*, 9953−9963.

(57) Frisch, M. J.; Trucks; H. B.; Schlegel, G. W.; Scuseria, G. E.; Robb, M. A.; Cheeseman, J. R.; Zakrzewski, V. G.; Montgomery, J., J. A.; Stratmann, R. E.; Burant, J. C.; Dapprich, S.; Millam, J. M.; Daniels, A. D.; Kudin, K. N.; Strain, M. C.; Farkas, O.; Tomasi, J.; Barone, V.; Cossi, M.; Cammi, R.; Mennucci, B.; Pomelli, C.; Adamo, C.; Clifford, S.; Ochterski, J.; Petersson, G. A.; Ayala, P. Y.; Cui, Q.; Morokuma, K.; Malick, D. K.; Rabuck, A. D.; Raghavachari, K.; Foresman, J. B.; Cioslowski, J.; Ortiz, J. V.; Baboul, A. G.; Stefanov, B. B.; Liu, G.; Liashenko, A.; Piskorz, P.; Komaromi, I.; Gomperts, R.; Martin, R. L.; Fox, D. J.; Keith, T.; Al-Laham, M. A.; Peng, C. Y.; Nanayakkara, A.; Gonzalez, C.; Challacombe, M.; Gill, P. M. W.; Johnson, B.; Chen, W.; Wong, M. W.; Andres, J. L.; Gonzalez, C.; Head-Gordon, M.; Replogle, E. S.; Pople, J. A. *Gaussian 98, Revision A.7*; Gaussian, Inc.: Pittsburgh, PA, 1998.

(58) Itoh, S. *Diamond Films Technol.* **1997**, *7*, 195−209.

(59) Nozaki, H.; Itoh, S. *Phys. Rev. B* **1996**, *53*, 14161−14170.

(60) Nozaki, H.; Itoh, S. *Physica B* **1996**, *220*, 487−489.

(61) Nozaki, H.; Itoh, S. *J. Phys. Chem. Solids* **1996**, *57*, 41−49.

(62) Tateyama, Y.; Ogitsu, T.; Kusakabe, K.; Tsuneyuki, S.; Itoh, S. *Phys. Rev. B* **1997**, *55*, 10161−10164.

(63) Wibbelt, M.; Kohl, H.; Kohler-Redlich, P. *Phys. Rev B* **1999**, *59*, 11739−11745.

(64) Blase, X.; Charlier, J. C.; De Vita, A.; Car, R. *Appl. Phys. A* **1999**, *68*, 293−300.